

Microarray analysis of micro-ribonucleic acid expression in primary immunoglobulin A nephropathy

Yong Dai, MD, PhD, Weiguo Sui, MOM, Huijuan Lan, MOM, Qiang Yan, MOM, He Huang, MB, Yuanshuai Huang, PhD.

ABSTRACT

الأهداف: لاستكشاف العلاقة بين اعتلال الجلوبين المناعي (A)، الكلوي الأولي (IgAN)، والتحليل المنظم الصغير لظهور حمض ريبيونيكليك (miRNA).

الطريقة: قمنا بتحليل ظهور ملفات حمض ريبيونيكليك (miRNA) في عينات كلوية من 11 (IgAN) مريضاً، و3 كمجموعة تحكم، بمركز زراعة الكلى والتنقية الدموية لـ 181 مستشفى بالصين، خلال الفترة ما بين مايو 2007 وحتى أكتوبر 2007. باستعمال التحليل المنظم المصغر لحمض ريبيونيكليك (miRNA) والمحتوي على التسلسلات الكاملة للإنسان البالغ وحمض ريبيونيكليك (miRNA).

النتائج: حددت الدراسة 132 ظهور لحمض ريبيونيكليك (miRNA) في العينات الكلوية، منها 31 حمض ريبيونيكليك (miRNA) منخفض التنظيم، و35 مرتفع التنظيم في عينات اعتلال الجلوبين المناعي الكلوي الأولي. تم تأكيد النتائج بواسطة اختبارات تفاعل سلسلة الحمائر الناقلة (RT-PCR) للوقت الحقيقي.

خاتمة: قد تساعد دراستنا في إيضاح الآلية الخلوية المتعلقة في المرض ومنشأة لاعتلال الجلوبين المناعي الكلوي الأولي (IgAN). يخدم حمض ريبيونيكليك (miRNA) بشكل أساسي كعلامة تشخيص حيوية للاعتلال الكلوي للجولبين المناعي الأولي (IgAN).

Objective: To explore the relationship between immunoglobulin A nephropathy (IgAN) and microRNA (miRNA).

Methods: We analyzed the miRNA expression profiles in renal biopsies from 11 IgAN patients and 3 controls at the Kidney Transplantation and Hemo Purification Center of 181 Hospital, China, from May to October 2007, using a mammalian miRNA microarray containing whole human mature and precursor miRNA sequences.

Results: This study identified 132 miRNAs in renal samples, of which 31 miRNAs down-regulated and 35 miRNAs up-regulated in IgAN biopsies. The chip

results were confirmed by northern blot analysis and by quantitative real-time polymerase chain reaction (RT-PCR) tests.

Conclusion: Our study may help clarify the molecular mechanisms involved in the pathogenesis of IgAN, and miRNAs potentially serve as a novel diagnostic biomarker of IgAN.

Saudi Med J 2008; Vol. 29 (10): 1388-1393

From the Clinical Medical Research Center (Dai), The Second Clinical Medical College, Jinan University, Shenzhen People's Hospital, Guangdong Province, and the Kidney Transplantation and Hemo Purification Center (Sui, Lan, Yan, Huang H), Hospital of Guilin, Guangxi Province, and the Laboratory Medicine (Huang Y), Key Laboratory of the Laboratory Medical Diagnostics, Ministry of Education, Chongqing Medical University, Chongqing, China.

Received 13th July 2008. Accepted 17th September 2008.

Address correspondence and reprint request to: Dr. Yuanshuai Huang, Key Laboratory of the Laboratory of Medical Diagnostics, Ministry of Education, Chongqing Medical University, Chongqing 400016, China. Tel/Fax. +86 (23) 68485005. E-mail: hys@live.cn

Primary immunoglobulin A nephropathy (IgAN) is one of the most frequent glomerulonephritides in developed countries, which were first described by Berger and Hinglais in 1968.¹ Primary IgAN is the main cause of end-stage renal disease in patients with primary glomerular disease, which requires renal-replacement therapy.² Given its frequency and significance, there should be a consensus on which treatment strategy is optimal for patients with IgAN.³ Until now, the pathogenesis of IgAN remains obscure, but new concepts have emerged during the last decade. Several work had been carried out in searching for the best prediction indices, such as circulating immunoglobulin A1 (IgA) molecules deficient in galactose (Gal),^{4,5} Gal-deficient IgA1,^{6,7} IgA-containing immune complexes,⁸ and serum secretory IgA were detected in patients with IgAN.⁹ However, none of them had been used in

clinical practice. Although specific therapy for IgAN is urgently required, the etiopathogenesis of IgAN remains unclear. Suzuki et al¹⁰ identified the susceptibility genes and examine their roles in the pathogenesis of IgAN by a genome-wide scan using the ddY mouse model. Genome-wide linkage analysis in 30 multiplex kindreds has demonstrated linkage of IgAN to 6q22-23.¹¹ Although various methods had been utilized in detecting the quantities of IgA, there is still no obvious candidate genes and biomarkers for IgAN. Studies conducted during the past 3 decades have identified many abnormalities in IgAN. Recent studies also examined the roles of abnormalities in the IgA molecule itself, such as negative charge and poor glycosylation, and some of IgA receptors, in the pathogenesis of IgAN.¹²⁻¹⁵ Therefore, a new approach is needed for the elucidation of etiopathogenesis of IgAN. MicroRNAs (miRNAs) are about 22-nucleotide, short, noncoding ribonucleic acids (RNA's) that are thought to regulate gene expression through sequence-specific base pairing with the 3'-untranslated region (3'-UTR) of target messenger ribonucleic acids (mRNAs). Hundreds of miRNAs have been identified in worms, flies, fish, frogs, mammals, and flowering plants using molecular cloning and bioinformatics prediction strategies.¹⁶ Since the discovery of the first miRNAs lin-4 and let-7 in *Caenorhabditis elegans* in 1993,¹⁷ at least 3420 miRNA genes in diverse organisms were identified. In recent years, several articles have been published showing a probable link between miRNAs and cancer,^{18,19} fragile X syndrome,²⁰ spinal muscular atrophy,²¹ DiGeorge syndrome,²² and systemic lupus erythematosus.²³ MicroRNAs have also been shown to regulate insulin secretion.²⁴ These studies represent the beginning links between miRNAs and human disease. Further investigations are likely to reveal the involvement of additional miRNAs and their targets in simple and complex genetic diseases. Understanding the mechanisms that contribute to primary IgAN, and find biomarkers to anticipate primary IgAN will be of great value for the development of improved nephropathy treatment strategies. Until now, there is no report of primary IgAN from the aspect of miRNAs. In our study, we compared the levels of miRNA expression in renal biopsies of primary IgAN between the normal samples, and try to reveal the relation between miRNA and primary IgAN.

Methods. We studied the biopsies of 11 IgAN patients at the Kidney Transplantation and Hemo Purification Center of 181 Hospital, China during the period May to October 2007. There were 8 men and 3 women aged 16-57 years (mean: 29 years). The patients' biopsies had shown 18 glomeruli on average, based on light microscopic findings, and slight-

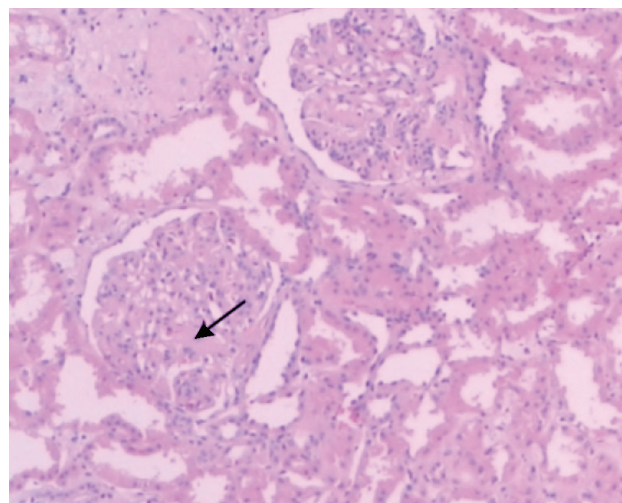


Figure 1 - Light microscopic examination for immunoglobulin A nephropathy (IgAN) biopsy (Hematoxylin and eosin stain, x400).

midrange mesangial proliferative glomerulonephritis (MesPGN) (Figure 1) according to Lee et al²⁵ grading system. There were no glomerular sclerosis (GS), glomerular atrophy, and sacculus proprius accretion. The interstitial inflammation and fibrosis were not obvious under light microscopic. Based on immunofluorescence microscopic observations, all samples exhibited more dominant mesangial deposits of IgA than of IgG and IgM with complement component 3 (c3) weakly positive, protein subunit of complement I and complement component 4 (c4) negative. Renal biopsies were performed based on clinical indication with ultrasound guidance, using the BIOPTYo instrument. The samples were renal cortex, obtained from aspiration-needle biopsy. All patients' diagnosis was confirmed by histology tests. The 3 samples for control group were renal cortex taken from resection operation of renal tumor, which is located far from the tumor tissue, and tissue structures were normal through light microscope checking. A written informed consent was obtained from all subjects or their guardians. The use of biopsy material for further studies beyond routine diagnosis was approved by the local ethics committee. This study was also performed according to the guidelines of Chongqing Medical University, which abides by the Helsinki Declaration on ethical principles for medical research involving human subjects.

Histological analysis. Biopsy material was immediately fixed in 10% phosphate-buffered paraformaldehyde, and stored at 4°C. After fixation, biopsies dehydrated through ascending ethanol series were embedded in EPON 812. The serial semi-thin sections (0.5 µm thick) were cut on a Reichert Ultracut

Table 1 - Reverse-transcribe and QRT-PCR primers.

| Gene name | QRT-PCR primers | Anneal temperature (°C) | Product length (bp) |
|-------------|---|-------------------------|---------------------|
| U6 | F:5' GCTTCGGCAGCACATATACTAAAAT 3' R:5' CGCTTCACGAATTTGCGTGTTCAT 3' | 60 | 89 |
| hsa-miR-637 | F:5' ACTGGGGGCTTTTCGGG R:5'AGTGCGTGTCTGGAGTC3' | 60 | 58 |
| hsa-miR-492 | F:5' GAGGACCTGCGGGACAA3' R:5'AGTGCGTGTCTGGAGTC3' | 60 | 62 |

Bp - base pair, QRT-PCR - quantitative reverse transcriptase polymerase chain reaction

Emicrotome. Resin was removed by treatment of sections with sodium methoxide prior to rehydration and immuno-staining as previously described.

Preparation of renal tissue samples. Aspiration-needle biopsy or renal cortex pieces (<0.3 x 0.3 x 0.3 mm³) obtained after nephrectomizing was immediately washed by 0.9% NaCl (RNase-free), quickly dipped in RNase Inhibitor (Epicentre, Mexico, USA) according to the manufacturer's instructions. After storing in 4°C overnight, the depressor was removed from the biopsies, and the biopsies were stored in -80°C for further test.

MicroRNA isolation. Total RNA was extracted from renal cortex pieces using Trizol (Invitrogen, California, USA) according to the manufacturer's instructions. The concentration and quality of RNA were measured by the UV absorbance at 260 nm and 280 nm (A₂₆₀/A₂₈₀), and checked by gel electrophoresis. All RNA was mixed in each sample group, and used for miRNA isolation and quantitative real-time polymerase chain reaction (QRT-PCR) verification. MicroRNA isolation was carried out from the total RNA using mirVana™ miRNA isolation kit (Ambion, Austin, Texas, USA) according to the manufacturer's instructions.

MicroRNA microarray. Locked nucleic acid modified capture probes were bought from Exiqon corporation of Denmark. MicroRNA microarray composes of 455 human miRNAs, 236 rat miRNAs, 344 mouse miRNAs, can detect all human miRNAs, rat miRNA, mouse miRNAs, and other species miRNAs in miRNA Sanger base (release 8.1). We used a novel microarray platform (miChip) that accurately and sensitively monitors the expression of miRNAs without prior need for RNA size fractionation and/or amplification and that can discriminate among closely related miRNA family members.

MicroRNA microarray analysis. MicroRNA was labeled by miRCURY™ Array Labelling kit (Cat #208032, Exiqon, Denmark) then concentrated the labeled sample by RNeasy Mini Kit (Cat #74104,

Qiagen, Germany) according to the manual. Hy3™ fluorescent label was used for dyeing. The hybridization was carried out according to the manufacturers instructions, 635 nm laser was used to scan the slide using the Genepix 4000B, and data analyzed by Genepix Pro 6.0. Hybridization was carried out twice on 2 different days.

Data analysis. Signal intensities for each spot were analyzed and calculated by the Image Quant 5.0 (Amersham Pharmacia Biotech Ltd., USA and Array vision 6.0 (Imaging Research Ltd., USA. Signal intensities for each spot were scanned and calculated by subtracting local background (based on the median intensity of the area surrounding each spot) from total intensities. An average value of the 2 spot replicates of each miRNA was generated after data transformation (to convert any negative value to 0.01), normalization was performed by using a per-chip 50th percentile method that normalizes each chip on its median, allowing comparison among chips. To highlight miRNAs that characterize each group, a per-gene on median normalization was performed, which normalizes the expression of every miRNA on its median among samples.

Quantitative real-time PCR verification of miRNA microarray results. Ribonucleic acid was reverse transcribed to complementary DNA with gene-specific primers. Quantitative real-time polymerase chain reaction primers are listed in Table 1, and cycle parameters for the PCR reaction was 95°C for 15 minutes, followed by 40 cycles of a denaturing step at 95°C for 10 seconds, and an annealing/extension step at 60°C for 60 seconds. All reactions were run in triplicate. The relative amount of each miRNA to U6 RNA was described by using the equation $2^{-\Delta Ct}$, where $\Delta Ct = (Ct_{miRNA} - Ct_{U6})$. The miRNAs analyses were hsa-miR-637 and hsa-miR-492.

Results. The quantity and quality of the RNA samples in IgAN and normal control (NC) group

Table 2 - Sixty-five MiRNAs with significant different expression levels detected in both immunoglobulin A nephropathy (IgAN) and normal control (NC) groups. Normalized hybridization signal of miRNAs identified in the microarray analysis are listed in this table.

| miRNA name | NC calibrated-sARVOL | IgAN calibrated-sARVOL | IgAN/NC ratio [†] |
|------------------------------------|----------------------|------------------------|----------------------------|
| <i>34 microRNAs down-regulated</i> | | | |
| hsa-miR-150_MM1 | 1.049 | 0.062 | 0.059 |
| hsa-miR-615 | 0.603 | 0.043 | 0.071 |
| hsa-miR-296 | 1.252 | 0.127 | 0.101 |
| hsa-miR-133a_MM1 | 0.215 | 0.022 | 0.102 |
| hsa-miR-637 | 0.682 | 0.074 | 0.108 |
| hsa-miR-133a-133b | 0.227 | 0.026 | 0.115 |
| hsa-miR-611 | 0.166 | 0.019 | 0.116 |
| hsa-miR-557 | 3.825 | 0.504 | 0.132 |
| hsa-miR-365 | 0.247 | 0.033 | 0.134 |
| hsa-miR-99a | 0.091 | 0.013 | 0.146 |
| hsa-miR-663 | 12.857 | 2.409 | 0.187 |
| hsa-miR-202_MM1 | 1.451 | 0.297 | 0.205 |
| hsa-miR-518b | 0.177 | 0.040 | 0.226 |
| hsa-miR-346 | 0.409 | 0.094 | 0.230 |
| hsa-miR-550 | 0.042 | 0.010 | 0.232 |
| hsa-miR-30d | 0.179 | 0.045 | 0.251 |
| hsa-miR-596 | 0.060 | 0.015 | 0.255 |
| hsa-miR-642 | 0.718 | 0.189 | 0.263 |
| hsa-miR-345_MM1 | 0.242 | 0.067 | 0.277 |
| hsa-miR-484 | 0.264 | 0.074 | 0.281 |
| hsa-miR-552 | 0.021 | 0.006 | 0.286 |
| hsa-miR-324-3p | 0.701 | 0.201 | 0.287 |
| hsa-miR-585 | 0.059 | 0.018 | 0.299 |
| hsa-miR-654 | 0.209 | 0.063 | 0.300 |
| hsa-miR-223 | 0.089 | 0.027 | 0.303 |
| hsa-miR-635 | 0.030 | 0.009 | 0.312 |
| hsa-miR-150 | 0.018 | 0.006 | 0.342 |
| hsa-miR-625 | 0.222 | 0.090 | 0.405 |
| hsa-miR-210 | 2.294 | 1.007 | 0.439 |
| hsa-let-7d_MM1 | 0.066 | 0.031 | 0.473 |
| hsa-miR-486 | 0.128 | 0.061 | 0.479 |
| <i>34 microRNAs up-regulated</i> | | | |
| hsa-miR-659 | 2.969 | 5.959 | 2.007 |
| hsa-miR-628 | 0.526 | 1.071 | 2.037 |
| hsa-miR-648 | 0.251 | 0.515 | 2.052 |
| hsa-miR-483 | 0.182 | 0.382 | 2.100 |
| hsa-miR-198 | 0.956 | 2.076 | 2.171 |
| hsa-miR-197_MM2 | 0.213 | 0.486 | 2.282 |
| hsa-miR-518c* | 3.540 | 8.433 | 2.383 |
| hsa-miR-526b | 0.128 | 0.311 | 2.423 |
| hsa-miR-23a | 0.028 | 0.068 | 2.474 |
| hsa-miR-302b*_MM1 | 1.306 | 3.314 | 2.538 |
| hsa-miR-600 | 0.010 | 0.028 | 2.780 |
| hsa-miR-657 | 0.010 | 0.028 | 2.984 |
| hsa-let-7a | 0.057 | 0.187 | 3.310 |
| hsa-miR-185 | 1.399 | 4.809 | 3.438 |
| hsa-miR-494 | 4.539 | 16.183 | 3.565 |
| hsa-miR-512-5p | 0.912 | 3.315 | 3.634 |
| hsa-miR-612 | 12.344 | 48.593 | 3.937 |
| hsa-miR-608 | 0.012 | 0.052 | 4.202 |
| hsa-miR-658 | 1.257 | 5.532 | 4.402 |
| hsa-miR-433 | 0.008 | 0.038 | 4.758 |
| hsa-miR-134 | 0.043 | 0.221 | 5.166 |
| hsa-miR-325_MM2 | 0.007 | 0.038 | 5.691 |
| hsa-miR-513 | 8.233 | 46.918 | 5.699 |
| hsa-miR-320 | 3.866 | 22.835 | 5.907 |
| hsa-miR-601 | 0.134 | 0.917 | 6.853 |
| hsa-miR-324-5p | 0.012 | 0.081 | 6.865 |
| hsa-miR-15b_MM1 | 0.003 | 0.026 | 7.433 |
| hsa-miR-208 | 0.002 | 0.016 | 7.943 |
| hsa-miR-622 | 0.005 | 0.040 | 8.109 |
| hsa-miR-30a-5p | 0.025 | 0.248 | 9.994 |
| hsa-miR-195 | 0.005 | 0.050 | 10.289 |
| hsa-miR-130b | 0.010 | 0.125 | 13.093 |
| hsa-miR-662 | 0.042 | 0.639 | 15.170 |
| hsa-miR-124a | 0.001 | 0.044 | 50.968 |

miRNAs are arranged according to the IgAN/NC ratio. †if the ratio was less than 2 or less than 0.5, the difference was significant. Calibrated-sARVOL - normalized fluorescence intensity with background subtracted

Table 3 - Sixty-six miRNAs without significant different expression levels detected valid expression in both immunoglobulin A nephropathy (IgAN) and normal control (NC) groups. Normalized hybridization signal of miRNAs identified in the microarray analysis are listed in this table.

| miRNA Name | NC calibrated-sARVOL | IgAN calibrated-sARVOL | IgAN/NC ratio [†] |
|--------------------|----------------------|------------------------|----------------------------|
| hsa-miR-452 | 1.141 | 0.580 | 0.508 |
| hsa-miR-381_MM1 | 0.212 | 0.109 | 0.512 |
| hsa-miR-125a_MM1 | 0.185 | 0.100 | 0.543 |
| hsa-miR-769-3p | 8.667 | 4.760 | 0.549 |
| hsa-miR-125b | 0.086 | 0.047 | 0.550 |
| hsa-miR-510 | 0.312 | 0.175 | 0.562 |
| hsa-miR-629 | 0.099 | 0.057 | 0.579 |
| hsa-miR-645 | 0.035 | 0.020 | 0.589 |
| hsa-miR-526c | 0.388 | 0.229 | 0.590 |
| hsa-miR-129 | 1.663 | 1.000 | 0.601 |
| hsa-miR-373* | 1.875 | 1.135 | 0.605 |
| hsa-miR-519d | 0.054 | 0.033 | 0.617 |
| hsa-miR-370 | 0.244 | 0.151 | 0.619 |
| hsa-miR-100_MM2 | 0.028 | 0.018 | 0.652 |
| hsa-miR-551a | 0.117 | 0.078 | 0.663 |
| hsa-miR-572 | 8.971 | 6.095 | 0.679 |
| hsa-miR-525*-524 | 0.018 | 0.013 | 0.706 |
| hsa-miR-107 | 0.161 | 0.117 | 0.723 |
| hsa-miR-527 | 0.464 | 0.363 | 0.781 |
| hsa-miR-500 | 0.711 | 0.559 | 0.787 |
| hsa-miR-602 | 5.027 | 4.094 | 0.814 |
| hsa-miR-214 | 0.331 | 0.276 | 0.835 |
| hsa-miR-198_MM2 | 2.871 | 2.430 | 0.846 |
| hsa-miR-451 | 0.021 | 0.018 | 0.853 |
| hsa-miR-520d* | 0.029 | 0.026 | 0.895 |
| hsa-miR-524* | 0.241 | 0.227 | 0.942 |
| hsa-miR-381 | 0.186 | 0.176 | 0.948 |
| hsa-miR-183_MM1 | 0.080 | 0.078 | 0.974 |
| hsa-miR-617 | 0.673 | 0.659 | 0.979 |
| hsa-miR-92b_MM2 | 0.389 | 0.404 | 1.037 |
| hsa-miR-202 | 1.252 | 1.350 | 1.079 |
| hsa-miR-103 | 0.115 | 0.127 | 1.109 |
| hsa-let-7b | 0.758 | 0.846 | 1.116 |
| hsa-miR-518f*-526a | 1.247 | 1.458 | 1.169 |
| hsa-miR-382 | 0.233 | 0.276 | 1.186 |
| hsa-let-7c | 1.353 | 1.615 | 1.193 |
| hsa-miR-423 | 0.082 | 0.099 | 1.207 |
| hsa-miR-197 | 0.086 | 0.105 | 1.217 |
| hsa-miR-525 | 0.745 | 0.921 | 1.236 |
| hsa-miR-17-3p_MM1 | 0.220 | 0.272 | 1.237 |
| hsa-miR-520a* | 0.055 | 0.069 | 1.255 |
| hsa-miR-519e* | 0.529 | 0.668 | 1.263 |
| hsa-miR-638 | 3.155 | 3.986 | 1.264 |
| hsa-miR-630 | 1.122 | 1.486 | 1.324 |
| hsa-miR-671 | 10.823 | 14.923 | 1.379 |
| hsa-miR-204_MM1 | 0.018 | 0.025 | 1.379 |
| hsa-miR-361 | 0.354 | 0.490 | 1.382 |
| hsa-miR-142-5p | 0.021 | 0.029 | 1.400 |
| hsa-miR-498 | 6.285 | 9.289 | 1.478 |
| hsa-miR-583 | 2.477 | 3.680 | 1.485 |
| hsa-miR-326 | 0.183 | 0.306 | 1.668 |
| hsa-miR-197_MM1 | 0.133 | 0.223 | 1.675 |
| hsa-miR-634 | 0.197 | 0.331 | 1.682 |
| hsa-miR-490 | 0.175 | 0.297 | 1.702 |
| hsa-miR-503 | 6.579 | 11.351 | 1.725 |
| hsa-miR-125a | 0.117 | 0.205 | 1.763 |
| hsa-let-7e | 0.124 | 0.221 | 1.781 |
| hsa-miR-184 | 0.072 | 0.129 | 1.784 |
| hsa-miR-492 | 6.066 | 10.835 | 1.786 |
| hsa-miR-200c | 0.013 | 0.023 | 1.817 |
| hsa-miR-516-5p | 0.173 | 0.320 | 1.848 |
| hsa-miR-584 | 1.153 | 2.132 | 1.849 |
| hsa-miR-330_MM1 | 0.037 | 0.069 | 1.859 |
| hsa-miR-623 | 6.407 | 12.416 | 1.938 |
| hsa-let-7a_MM1 | 0.048 | 0.095 | 1.989 |
| hsa-miR-575 | 0.008 | 0.017 | 1.997 |

miRNAs are arranged according to miRNA names. †if the ratio was less than 2 or less than 0.5, the difference was significant. Calibrated-sARVOL - normalized fluorescence intensity with background subtracted

were checked by gel electrophoresis (Figure 2), and absorbance at A260/280 ratio (in NC [1.85], IgAN [2]). The A260/280 ratio and gel electrophoresis results confirmed the good quality of RNA isolated. After normalization of the raw data, 131 miRNAs were detected in both groups with 65 of them differentially expressed by miRNA microarray, in which 31 miRNAs down-regulated, and 34 miRNAs up-regulated in absorbance ratio (AR) compared with the NC group (Table 2), while 66 miRNAs without significant different expression levels (Table 3). Microarray data are consistent with the QRT-PCR verification results (Table 4) for that the AR/NC ratio of hsa-miR-637 was 0.108, and hsa-miR-492 was 1.786 in microarray test, while in QRT-PCR test, ratio for hsa-miR-637 was 0.095, and hsa-miR-492 was 1.659, which was close.

Discussion. In the present study, we comprehensively isolated and analyzed miRNAs in the patients' tissue of primary IgAN and normal control, using miRNA

microarray analysis. This study identified 132 miRNAs in renal samples, of which 31 miRNAs down-regulated and 35 miRNAs up-regulated in IgAN biopsies. Immunoglobulin A neuropathy is a relatively newly recognized disease since described by Berger and Hinglais in 1968.¹ It is now generally known to be the most common form of primary glomerulonephritis throughout the world.²⁶⁻²⁸ Though many research on IgAN's pathogenesis and methods of treatment, Batra et al²⁹ hypothesized that the activated systemic homing cluster of differentiation 4 -T cells may direct the aberrant systemic pIgA production observed in IgAN.³⁰ Praga et al³⁰ treat IgAN with angiotensin-converting enzyme (ACE) inhibitors, and ACE had been reported as one susceptibility genes of IgAN). Until recently, there was no effective treatment available for patients with IgAN. Primary IgAN rate was different in different gender, race and location. Generally, male have high primary IgAN rate than female, the ratio was 2:1 in Japan, and 6:1 in northern Europe and the United States, and the lower prevalence in blacks than whites, and Asians. It indicated that primary IgAN were associate closely with gene. MicroRNA is the regulator of mRNA, indirectly regulates protein expression. The link between miRNAs and some human diseases has been proven. In this study, we apply miRNA microarray chip to analyze relationship between IgAN and miRNAs, which has not been studied before. From IgAN and normal control kidney biopsies, we identified 131 miRNAs, 65 of which were found with significantly different expression levels. For these 20 miRNAs, we can predict their targets with computational target predictions such as miRanda available at <http://www.microrna.org>, and mirBase available at <http://microrna.sanger.ac.uk/targets/v2/etc>.³¹ For example, the up-regulated hsa-miR-125a, 1180 hits was found in the target predicting database. The individual miRNA variation between patients may be difficult to detect with no significance, due to random changes that may exist in each patient. In our study, all RNA from each sample group was merged so that the individual

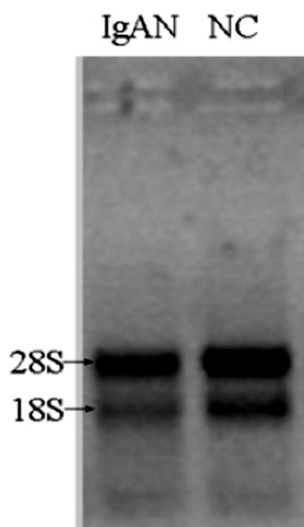


Figure 2 - Gel electrophoresis check of pooled total RNA from immunoglobulin A nephropathy (IgAN) and normal control (NC) samples.

Table 4 - Quantitative reverse transcriptase-polymerase chain reaction confirmation data.

| Samples | Ct _{U6} | Ct _{miRNA} | $\Delta Ct = (Ct_{miRNA} - Ct_{U6})$ | $Ct_{(IgAN-NC)} = \Delta Ct_{IgAN} - \Delta Ct_{NC}$ | $2^{-Ct_{(IgAN-NC)}}$ | IgAN/NC ratio |
|--------------------|------------------|---------------------|--------------------------------------|--|-----------------------|---------------|
| <i>hsa-miR-637</i> | | | | | | 0.095 |
| NC | 13.06 | 19.86 | 6.8 | 0 | 1 | |
| IgAN | 12.91 | 23.11 | 10.2 | 3.4 | 0.095 | |
| <i>hsa-miR-492</i> | | | | | | 1.659 |
| NC | 13.06 | 16.93 | 3.87 | 0 | 1 | |
| IgAN | 12.91 | 16.05 | 3.14 | -0.73 | 1.659 | |

Ct - Ct value, Ct is a cycle threshold, NC - normal control group, IgAN - immunoglobulin A nephropathy

difference between subjects is eliminated. The aim of this study is to reveal the relationship between IgAN and miRNAs to the public, expecting to draw other research groups' attention to this area. The lack of functional research on IgAN related miRNAs we detected, is the limitation of this study.

Taken together, we identified the 65 miRNAs differentially expressed in IgAN whose expression profiling may provide a useful clue for the pathophysiology research of IgAN. Our work indicates that miRNAs are potential diagnosis biomarkers and probable factors involved in the pathogenesis of IgAN. Further investigation is needed to clarify the roles of identified miRNAs in the pathogenesis of IgAN. Our study of miRNAs may lead to finding novel methods to diagnosis, treat, and prevent IgAN, and to provide a novel researching method for it.

References

- Berger J, Hinglais N. Les depots intercapillaires d'IgA-IgG. *J Urol Nephrol* 1968; 74: 694-695.
- Briganti EM, Dowling J, Finlay M, Hill PA, Jones CL, Kincaid-Smith PS, et al. The incidence of biopsy-proven glomerulonephritis in Australia. *Nephrol Dial Transplant* 2001; 16: 1364-1367.
- Ballardie FW. IgA nephropathy treatment 25 years on: Can we halt progression? The evidence base. *Nephrol Dial Transplant* 2004; 19: 1041-1046.
- Tomana M, Matousovic K, Julian BA, Radl J, Konecny K, Mestecky J. Galactose-deficient IgA1 in sera of IgA nephropathy patients is present in complexes with IgG. *Kidney Int* 1997; 52: 509-516.
- Barratt J, Feehally J. IgA nephropathy. *J Am Soc Nephrol* 2005; 86: 2088-2097.
- Allen AC, Bailey EM, Brenchley PE, Buck KS, Barratt J, Feehally J. Mesangial IgA1 in IgA nephropathy exhibits aberrant O-glycosylation: observation in three patients. *Kidney Int* 2001; 60: 969-973.
- Hiki Y, Odani H, Takahashi M, Yasuda Y, Nishimoto A, Iwase H, et al. Mass spectrometry proves under-O-galactosylation of glomerular IgA1 in IgA nephropathy. *Kidney Int* 2001; 59: 1077-1085.
- Matousovic K, Novak J, Yanagihara T, Tomana M, Moldoveanu Z, Kulhavy R, et al. IgA-containing immune complexes in the urine of IgA nephropathy patients. *Nephrol Dial Transplant* 2006; 21: 2478-2484.
- Zhang JJ, Xu LX, Liu G, Zhao MH, Wang HY. The level of serum secretory IgA of patients with IgA nephropathy is elevated and associated with pathological phenotypes. *Nephrol Dial Transplant* 2007; 10: 1093-1099.
- Suzuki H, Suzuki Y, Yamanaka T, Hirose S, Nishimura H, Toei J, et al. Genome-Wide Scan in a Novel IgA Nephropathy Model Identifies a Susceptibility Locus on Murine Chromosome 10, in a Region Syntenic to Human IGAN1 on Chromosome 6q22-23. *J Am Soc Nephrol* 2005; 16: 1289-1299.
- Gharavi AG, Yan Y, Scolari F, Schena FP, Frasca GM, Ghiggeri GM, et al. IgA nephropathy, the most common cause of glomerulonephritis, is linked to 6q22-23. *Nat Genet* 2000; 26: 354-357.
- D'Amico G. Pathogenesis of immunoglobulin A nephropathy. *Curr Opin Nephrol Hypertens* 1998; 7: 247-250.
- Hiki Y, Kokubo T, Iwase H, Masaki Y, Sano T, Tanaka A, et al. Underglycosylation of IgA1 hinge plays a certain role for its glomerular deposition in IgA nephropathy. *J Am Soc Nephrol* 1999; 10: 760-769.
- Tomana M, Novak J, Julian BA, Matousovic K, Konecny K, Mestecky J. Circulating immune complexes in IgA nephropathy consist of IgA1 with galactose-deficient hinge region and antiglycan antibodies. *J Clin Invest* 1999; 104: 73-81.
- Novak J, Vu HL, Novak L, Julian BA, Mestecky J, Tomana M. Interactions of human mesangial cells with IgA and IgA-containing immune complexes. *Kidney Int* 2002; 62: 465-475.
- Lagos-Quintana M, Rauhut R, Lendeckel W, Tuschl T. Identification of novel genes coding for small expressed RNAs. *Science* 2001; 294: 853-858.
- Lee RC, Feinbaum RL, Ambros V. The C. elegans heterochronic gene lin-4 encodes small RNAs with antisense complementarity to lin-14. *Cell* 1993; 75: 843-854.
- Calin GA, Croce CM. MicroRNA-cancer connection: the beginning of a new tale. *Cancer Res* 2006; 66: 7390-7394.
- Yanaihara N, Caplen N, Bowman E, Seike M, Kumamoto K, Yi M, et al. Unique microRNA molecular profiles in lung cancer diagnosis and prognosis. *Cancer Cell* 2006; 9: 189-198.
- Jin P, Alisch RS, Warren ST. RNA and microRNAs in fragile X mental retardation. *Nat Cell Biol* 2004; 6: 1048-1053.
- Mourelatos Z, Dostie J, Paushkin S, Sharma A, Charroux B, Abel L. miRNPs: a novel class of ribonucleoproteins containing numerous microRNAs. *Genes Dev* 2002; 16: 720-728.
- Landthaler M, Yalcin A, Tuschl T. The human DiGeorge syndrome critical region gene 8 and its D. melanogaster homolog are required for miRNA biogenesis. *Curr Biol* 2004; 14: 2162-2167.
- Dai Y, Huang YS, Tang M, Lv TY, Hu CX, Tan YH, et al. Microarray analysis of microRNA expression in peripheral blood cells of systemic lupus erythematosus patients. *Lupus* 2007; 16: 939-946.
- Poy MN, Eliasson L, Krutzfeldt J, Kuwajima S, Ma X, Macdonald PE, et al. A pancreatic islet-specific microRNA regulates insulin secretion. *Nature* 2004; 432: 235-240.
- Lee HS, Lee MS, Lee SM, Lee SY, Lee ES, Lee EY, et al. Histological grading of IgA nephropathy predicting renal outcome: revisiting HS Lee's glomerular grading system. *Nephrol Dial Transplant* 2005; 20: 342-348.
- Donadio JV, Grande JP. IgA nephropathy. *N Engl J Med* 2002; 347: 738-748.
- Julian BA, Waldo FB, Rifai A, Mestecky J. IgA nephropathy, the most common glomerulonephritis worldwide: a neglected disease in the United States? *Am J Med* 1988; 84: 129-132.
- Levy M, Berger J. Worldwide perspective of IgA nephropathy. *Am J Kidney Dis* 1988; 12: 340-347.
- Batra A, Smith AC, Feehally J, Barratt J. T-cell homing receptor expression in IgA nephropathy. *Nephrol Dial Transplant* 2007; 22: 2540-2548.
- Praga M, Gutiérrez E, González E, Morales E, Hernández E. Treatment of IgA Nephropathy with ACE Inhibitors: a randomized and controlled trial. *J Am Soc Nephrol* 2003; 14: 1578-1583.
- Rajewsky N. microRNA target predictions in animals. *Nat Genet* 2006; 38 Suppl: S8-S13.